AD-A231 768

REPORT DOCUMENTATION PAGE

Form Approved
OMB No. 0704-0188

Public reporting burden for this collection of information is estimated to average 1 hour per response, including the time for reviewing instructions, searching existing data sources, gathering and maintaining the data needed, and completing and reviewing the collection of information. Send comments regarding this burden estimate or any other aspect of this collection of information, including suggestions for reducing this burden, to Washington Headquarters Services, Directorate for Information Operations and Reports, 1215 Jefferson Davis Highway, Suite 1204, Arlington, VA 22202-4302, and to the Office of Management and Budget, Paperwork Reduction Project (0704-0188), Washington, DC 20503.

1. Agency Use Only *(Leave blank).*	2. Report Date.	3. Report Type and Dates Covered.
	October 1989	

4. Title and Subtitle.
Arctic Studies with Coupled Ice-Ocean Models

5. Funding Numbers.
Program Element No. 63207N
Project No. 00513
Task No. 999
Accession No. DN894428

6. Author(s).
Alex Warn-Varnas*, Rick Allard and Steve Piacsek*

7. Performing Organization Name(s) and Address(es).
*SACLANT Undersea Research Center
La Spezia, Italia

8. Performing Organization Report Number.
AB 90:322:004

9. Sponsoring/Monitoring Agency Name(s) and Address(es).
Space and Naval Warfare Systems Command
Code PDW 106-8
Washington, DC 20361

10. Sponsoring/Monitoring Agency Report Number.
AB 90:322:004

11. Supplementary Notes.
Berkeley Research Associates
Springfield, VA

DTIC
ELECTE
FEB 06 1991
S D
D

12a. Distribution/Availability Statement.
Approved for public release; distribution is unlimited.

12b. Distribution Code.

13. Abstract *(Maximum 200 words).*

The upper ocean is modeled in the framework of a three dimensional mixed-layer approximation and is coupled to the Hiber thermodynamic dynamic ice model. Two different modeling approaches are used for theinterior ocean. In one, the geostrophic velocity is obtained from an inverse, Beta-spiral, type of model. In another, the barotropic velocity is calculated prognostically. Topography is included in both approaches. The model is initialized form Levitus climatology and is forced by NOGAPS atmospheric forcing. Studies of diurnal and seasonal regimes are performed. The nature of the boundary layer under ice, in the marginal ice zone. and open water is analyzed. Transmission of wind stress through the ice is considered. The resultant Ekman pumping and the forcings of the interior ocean are calculated. In the Greenland and Norwegian Sea areas, major changes in the behavior of the upper ocean are observed from the Arctic Basin outwards. Deep neutrally stable mixed layers tend to occur outside the MIZ. The heat and salt budgets of these regions are computed.

14. Subject Terms.			15. Number of Pages.
Sea Ice Forecasting, Sea Ice Models, Sea Ice Analysis			7
			16. Price Code.
17. Security Classification of Report.	18. Security Classification of This Page.	19. Security Classification of Abstract.	20. Limitation of Abstract.
Unclassified	Unclassified	Unclassified	SAR

NSN 7540-01-280-5500

Standard Form 298 (Rev. 2-89)
Prescribed by ANSI Std. 239-18
298-102

91 2 05 059

Arctic Studies with Coupled Ice-Ocean Models

Alex Warn-Varnas[+], Rick Allard[*]
and
Steve Piacsek[+]

[+] - SACLANT Undersea Research Center
La Spezia, Italia
[*] - Berkeley Research Associates
Springfield, VA

December 6, 1989

1 Introduction

Various physical phenomena are observed to occur in the arctic and its subregions. The most noted one is the sea ice itself that reflects a phase change of sea water in response to atmospheric cooling. Once formed it acts as a insulator between the ocean and the ice. The resultant oceanic structure beneath the ice acquires a distinct characteristic relative to the open water regions. Temperatures beneath the ice tend to be near freezing, while the salinity and with it the mixed layer dynamics are controlled by the freezing and melting of the ice through the subsequent brine injection or dilution. The mixed layer depths themselves tend to vary from 30 to 70 meters under the ice.

The arctic ocean can be compartmentalized naturally into different regions, depending on the predominant processes. In the upper layer, turbulent mixing and Coriolis effects are equally important and as a result, this layer has Ekman-like dynamics. In the interior the pressure gradients tend to balance the Coriolis force, resulting in a quasi-geostrophic flow. At the bottom, there is a benthic boundary layer that has Ekman type dynamics and is forced by the interior flow. A lateral transport of vorticity proceeds from the basin boundaries toward the interior.

In such an approach the resulting oceanic velocity can be thought of as a superposition of velocities arising from the various regions: top, interior, and bottom. We exploit this property by essentially solving separate models for the various regions of the ocean, with coupling between them.

The upper ocean is modelled in the framework of a three-dimensional mixed layer approximation, and is coupled to the Hibler thermodynamic- dynamic ice model. Two different modelling approaches are used for the interior ocean. In one, the geostrophic velocity is obtained from an inverse, β-spiral type model. In another, the barotropic velocity is calculated prognostically. Topography is included in both approaches.

The seasonal and regional behaviors of the ice-ocean structure is studied, along with the temperature and salinity distributions (under the ice, in the MIZ, and in the open water) In addition, the nature of the mixing processes and their effect on the upper

A-1

ocean heat and salt budgets are anlyzed. Finally, we compare the ice edge locations against analysed results derived from remote sensing and some in-situ reports.

The seasonal behavior of the barotropic flow has also been modelled in the Arctic, including the Greenland and Norwegian Sea basins. The time behavior of the associated transports has also been studied.

2 Modeling Approach

For ice representation the dynamic-thermodynamic model of Hibler (1979, 1980) was used. In this model the momentum balance of the ice is expressed as

$$m(D\vec{u}/dt) = mf(\vec{k} \times \vec{v}) + \vec{\tau_a} + \vec{\tau_b} - mg\nabla H + \vec{F} \tag{1}$$

where m is the ice mass per unit area, $\vec{u}$ is the ice velocity, f is the Coriolis parameter, $\vec{\tau_a}$ and $\vec{\tau_b}$ are the atmospheric and bottom stresses, H is the sea surface dynamic height, and $\vec{F}$ is the force due to variation in the internal ice stress.

The ice thickness and compactness equations are treated as in Hibler (1979), together with the Semtner (1976) thermodynamics model for ice growth and decay.

The equations describing the upper mixed region are as follows

$$\vartheta T/\vartheta t = \vartheta/\vartheta z(-\overline{w'T'} + \kappa(\vartheta T/\vartheta z)) + (1/\rho_w c)(\vartheta F/\vartheta z) - \nabla \cdot (\vec{u}T) + A\nabla^2 T) \tag{2}$$

$$\vartheta S/\vartheta t = \vartheta/\vartheta z(-\overline{w'S'} + \kappa(\vartheta S/\vartheta z)) - \nabla \cdot (\vec{u}S) + A \cdot \nabla^2 S) \tag{3}$$

$$\vartheta u/\vartheta t = \vartheta/\vartheta z(-\overline{w'u'} + \kappa(\vartheta u/\vartheta z)) + fv - Du \tag{4}$$

$$\vartheta v/\vartheta t = \vartheta/\vartheta z(-\overline{w'v'} + \kappa(\vartheta v/\vartheta z)) - fu - Dv \tag{5}$$

where T is the mean temperature, S is the mean salinity, u, v and w the x-, y-, and z-components of an advective oceanic current velocity (to be defined later), F the downward flux of solar radiation, ρ_w a reference water density, c the specific heat of seawater, D a damping coefficient, κ an ambient diffusion coefficient, f the Coriolis parameter, A the horizontal eddy diffusion coefficient, t the time, and z the vertical coordinate (positive upward from the level sea surface). Primes indicate departure from the means. The advective terms are retained in the temperature and salinity equations, but neglected in the momentum equations., based on a scale analysis.

The advection current is given by

$$u = u_i + u_g, v = v_i + v_g, w = w_i \tag{6}$$

where the u_i and v_i are components of the instantaneous wind-drift current, w_i is the vertical motion resulting from the divergence of the $\vec{u_i}$ field, and u_g and v_g are components of a geostrophic current.

The Level-2 turbulence closure method of Mellor and Yamada (1974) is used to parametrize the vertical eddy fluxes of temperature, salinity and momentum. The geostrophic velocity is calculated with a β-spiral type inverse method of Peggion (1988). The model assumes the usual hydrostatic and geostrophic approximations. Additional

constraints are imposed on the density field due to mass conservation and the topography. The resulting linear equations fitting all constraints to the data are solved through a minimization procedure.

The horizontal grid is shown in Figure 1. It is defined at equal intervals on the polar stereographic projection used for the domain, with a total resolution of 47x25 grid points, and a mean grid distance of $\sim$ 127 km. The vertical grid contains 17 levels and is stretched, with a resolution that varies from $5m$ near the surface to several hundred meters near the bottom. The resolution is designed to track variations in the mixed layer, mostly in middle latitudes.

The net flow (i.e. barotropic) model is formulated by integrating the equations from bottom to top, and taking its curl to eliminate the free surface gravity waves. The final equation is expressed in terms of the mass transport stream function Ψ and is as follows

$$\vartheta/\vartheta t(\nabla \cdot (1/H) \cdot \nabla)(\Psi - \Phi/f) = \nabla \cdot (\vec{\tau_0}/H) - (\beta/fh^2) \cdot (\vartheta(\Phi/H)/\vartheta x) \quad (7)$$

$$+ (\vartheta H/\vartheta x).(\vartheta\Phi/\vartheta y) - (\vartheta H/\vartheta y).(\vartheta\Phi/\vartheta x) + \nabla \cdot (A_h/H \cdot \nabla^2(\nabla\Psi)) \quad (8)$$

where $\vec{\tau_0} = \vec{\tau} - \vec{Q}$, and $\Phi = (g/H^2) \cdot \int z\sigma_z dz$. Here $\vec{\tau}$ is the surface stress, $\vec{Q}$ is the bottom torque, σ_z is the in-situ density anomaly, β is the NS variation of the Coriolis parameter, and A_h is the lateral viscosity.

3 Research Studies and Discussions

We began our modelling studies with the first approach described above, in which the ice and the upper ocean are represented prognostically and the interior ocean diagnostically. The model was initialized with temperatures and salinities taken from the Levitus climatology, and was forced by 12-hourly atmospheric fluxes derived from the NOGAPS global atmospheric prediction model of FNOC (Fleet Numerical Ocean Central in Monterey, CA). The integrations were performed for five years. At the end of this period the seasonal behavior has converged to a statistical equilibrium, such that the annual evolutions of the ice thickness and ice concentration have repeated themselves during the fourth and fifth year. Temperatures, salinities, and velocities behaved similarly. In the fourth year the average ice thickness for the month of December has evolved to the state shown in Figure 2. From the North slope towards the North Pole the ice thickness decreases, as expected from previous work. The NPOC (Navy Polar Ocean Center in Washington) analysis for ice edge location in the Barents and Greenland Seas is indicated in the figure. The disagreement in the Barents Sea we attribute to the weakness of the warm Norwegian current, as calculated by the diagnostic interior ocean model employing the (coarse resolution) Levitus climatology. Not enough heat is transported into the ice edge region. The disagreement near Greenland we attribute to similar problems with the Greenland Current.

In figures 3 and 4 we display the temperature and salinity along the transect shown in Figure 1, during the summer on day 216. Three distinct regions can be identified: under the ice, the MIZ, and the open water. Under the ice the stratification tends to be stronger than elsewhere.

During the summer the effects of the melting ice are manifested as lower salinities under the ice sheet due to salt dilution. In the winter months the opposite effect occurs. In the MIZ there is warm water where during the winter ice and well mixed colder water existed. In the open water we see the effects of the summer stratification of the surface

layers. In the winter they are well mixed. The salinity is high in the open water in the summer and winter, reflecting the presence of warm saline Atlantic water. In the MIZ there is warm water where during the winter ice and well mixed colder water prevailed.

In the upper ocean region, the velocity is a superposition of the Ekman, inertial, and geostrophic velocities. An example of it is shown in figure 5 at 2.5 meters during day 8 of the simulation. The observed patterns are controlled by the wind stress (transmitted through the ice and applied to the open water). The water movement follows the ice motion at an angle. The geostrophic velocity varies from a few cm/sec to about 10 cm/sec. Its patterns reflect the Beaufort gyre, the transpolar drift, and the Greenland and Norwegian currents. As mentioned before it is calculated diagnostically from the Levitus climotalogy in this approach.

As a next step in our development of models of increasing complexity, we have introduced a prognostic calculation of the barotropic ocean velocity. Topography is included in the formalism and is coupled to the density field via the JBAR representation. Our first aim was to study the evolution of the basic net flow gyres that would arise without coupling to the density field or the ice. For forcing we have used the 30-year climatological winds of Dr. John Walsh of the University of Illinois. We have converged the model to a steady state and studied the seasonal behavior of the gyres that evolved. In the winter an anti-cyclonic gyre developed in the Beafort Sea, together with cyclonic gyres in the Greenland-Norwegian and Barents Seas. These results are in agreement with Semtner(1987) who has also studied the circulation of the Arctic. In the summer two gyres have developed in the Arctic basin, an anticyclonic gyre in the Bering Sea side and a cyclonic gyre in the Barents Sea side (Figure 6). This supports the previously observed reversal of the ice drift in the summer in the Greenland and Canadian sections of the Arctic Basin. It is suggested that the climatological winds have a signature of the curl in them which corresponds to that of the circulation.

The transports of the permanent gyres exhibit a seasonal variation. The Greenland-Norwegian gyre has a maximum in the winter and a minimum in the summer. The Barents sea gyre has a similar behavior. The Beaufort sea gyre has a summer minimum with two maxima (Figure 7). This seasonal behavior agrees with Semtner (1987). Our magnitudes are, however, somewhat larger than his.

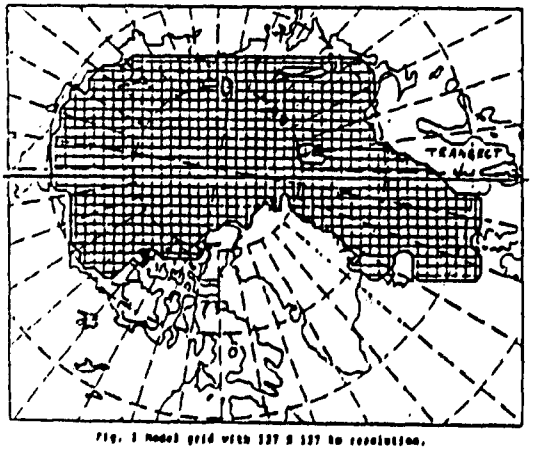

Fig. 1 Model grid with 127 x 127 km resolution.

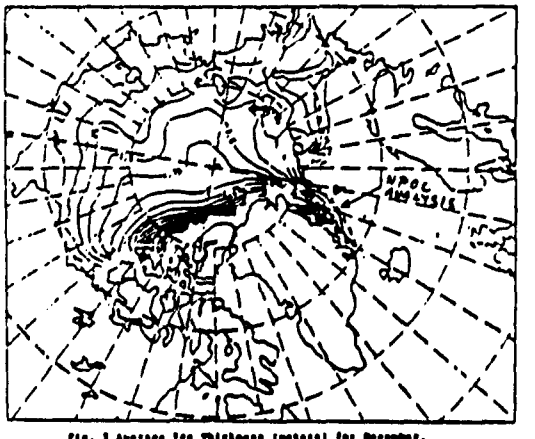

Fig. 2 Average ice thickness (meters) for December, (dotted line represents NPOL analysis)

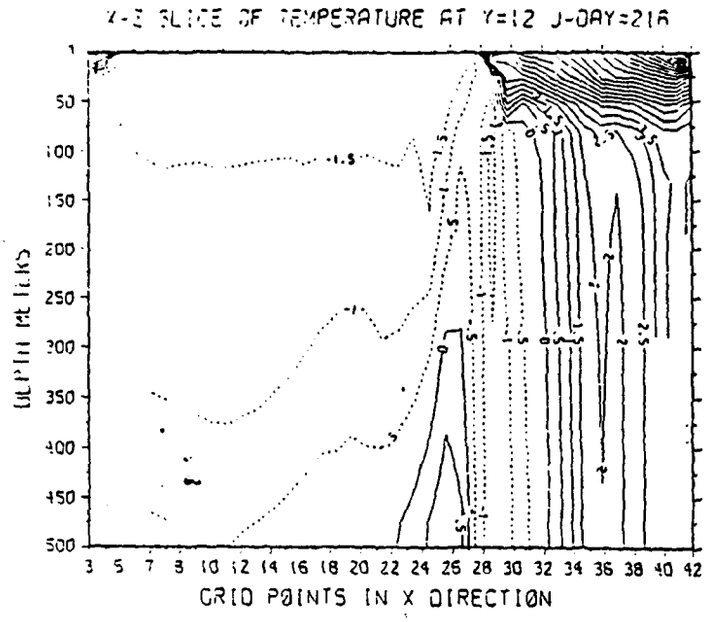

Fig. 3 Vertical Cross-Section of Temperature(°C) on day 216.

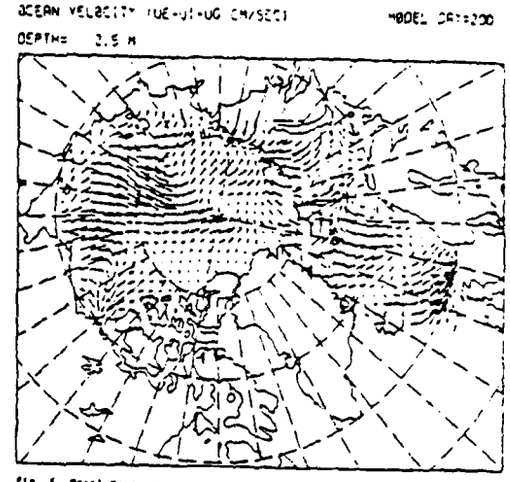

Fig. 5 Total Horizontal Velocity (Ekman, Inertial, and Geostrophic) in cm/sec on day 200 at 2.5 meters.

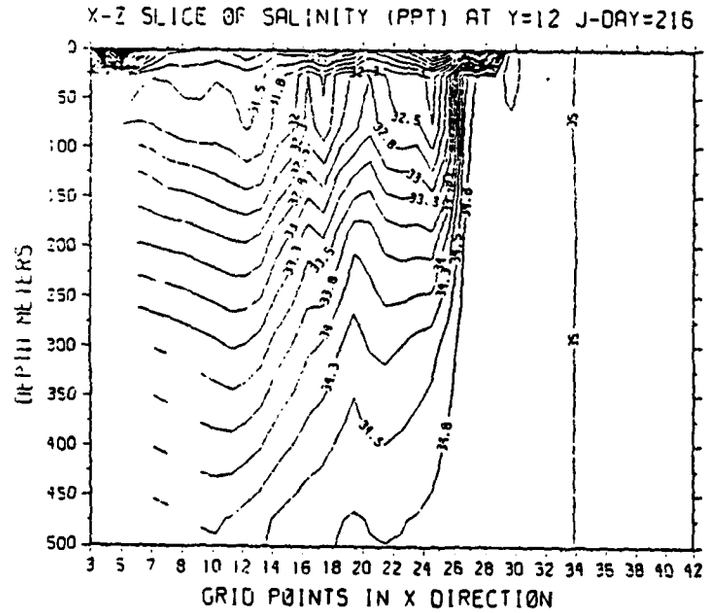

Fig. 4 Vertical Cross-Section of Salinity (PPT) on day 216.

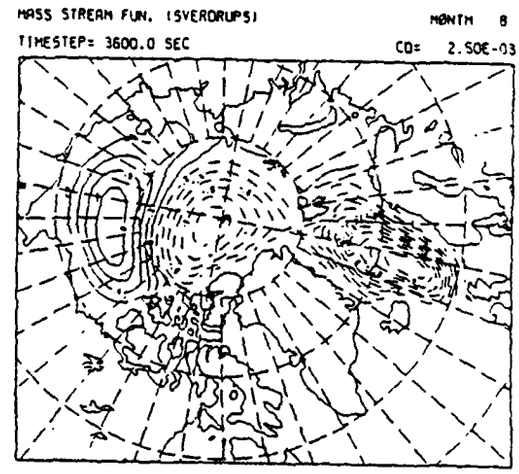

Fig.6 Mass Flow Stream function in Sverdrups for the month of August.